J. Geogr. Sci. 2020, 30(1): 3-17
DOI: https://doi.org/10.1007/s11442-020-1711-1

© 2020 Science Press Springer-Verlag

Scenarios of land cover in Eurasia under climate change

FAN Zemeng[1,2,3], BAI Ruyu[1,2], YUE Tianxiang[1,2,3]

1. State Key Laboratory of Resources and Environment Information System, Institute of Geographic Sciences and Natural Resources Research, CAS, Beijing 100101, China;
2. University of Chinese Academy of Sciences, Beijing 100049, China;
3. Jiangsu Center for Collaborative Innovation in Geographical Information Resource Development and Application, Nanjing 210023, China

Abstract: The method for surface modelling of land cover scenarios (SMLCS) has been improved to simulate the scenarios of land cover in Eurasia. On the basis of the observation monthly climatic data observed from 2127 weather stations in Eurasia during 1981–2010, the climatic scenarios data of RCP26, RCP45 and RCP85 scenarios released by CMIP5, and the land cover current data of Eurasia in 2010, the land cover scenarios of Eurasia were respectively simulated. The results show that most land cover types would generally have similar changing trends in the future, but with some difference in different periods under the three scenarios of RCP26, RCP45 and RCP85. Deciduous needleleaf forest, mixed forest, shrub land, wetlands and snow and ice would generally decrease in Eurasia during 2010–2100. Snow and ice would have the fastest decreasing rate that would decrease by 37.42% on average. Shrub land would have the slowest decreasing rate that would decrease by 5.65% on average. Water bodies would have the fastest increasing rate that would increase by 28.78% on average. Barren or sparsely vegetated land would have the slowest increasing rate that would increase by 0.76%. Moreover, the simulated results show that climate change would directly impact on land cover change in Eurasia.

Keywords: SMLCS, climate change; land cover; scenarios; Eurasia

1 Introduction

Land cover change, as a fundamental variable of earth surface, directly affects biogeochemical cycle, hydrological cycle, soil erosion and biological diversity (Chapin *et al*., 2000; Foley *et al*., 2005; Sala *et al*., 2000; Bolliger *et al*., 2011; Fan *et al*., 2013, 2015), and climate change also directly drives land cover change (Fu, 2003; Yue *et al*., 2007; Fan *et al*., 2015). Since the International Geosphere-Biosphere Program (IGBP) and International Human Dimensions Programme (IHDP) on global environmental change jointly proposed the

Received: 2018-06-15 **Accepted:** 2019-02-28
Foundation: National Key R&D Program of China, No.2017YFA0603702, No.2018YFC0507200; National Natural Science Foundation of China, No.41421001, No.41271406; Innovation Project of LREIS, No.O88RA600YA
Author: Fan Zemeng, PhD, specialized in ecological modelling and system simulation. E-mail: fanzm@lreis.ac.cn

research program of Land Use and Land Cover Change (LUCC) in 1995, many models have been developed for simulating land cover scenarios.

The IIASA land-use change model was developed to simulate the future scenarios of land use/cover by considering the socio-economic factor, biogeophysical driving force, and food policies (Fischer *et al*., 1996). Economic models were introduced to analyze land cover change on a regional scale (Ichinose and Otsubo, 2003). The Integrated Model to Assess the Greenhouse Effect (IMAGE), as a global integrated system model, was developed for simulating agricultural ecology process (Alcamo *et al*., 1994). The Conversion of Land Use and its Effects (CLUE) was developed within a framework of conversion of land use and its effects under assumptions (Verbrug *et al*., 1999, 2002, 2004). The Cellular Automata (CA) model was involved to simulate the urban land use scenarios (Clarke *et al*., 1997; Wu and Webster, 1998; Wu, 2002), and improved to downscale cultivated land and built-up land of the global land use datasets (Li *et al*., 2016). The Surface Modeling of Land Cover Scenarios (SMLCS) to simulate the change of land cover scenarios in China (Yue *et al*., 2007).

However, there are some limitations in these models. The IIASA land-use change model and economic models focus on addressing the question what is the change rate of land cover, but don't answers the questions where is the location of land cover changes. IMAGE land cover model focuses on the demand of agricultural land and ignores the effect of climate change on future land cover. CA land cover model is mainly used to simulate the land cover scenarios at an urban or river basin scale. At a large scale, CA land cover model only has been improved to downscale the agricultural land and built-up land of global land cover data. The early versions of the SMLCS model only can be used to simulate the land cover scenarios at a country scale (Fan *et al*., 2015). So, this paper aims to improved SMLCS model to simulate the land cover scenarios in Eurasia.

2 Data and Methods

2.1 Datasets

The basic datasets include the observation climatic data, climatic scenarios data and land cover data. The observation monthly climatic data has been collected from 2127 weather observation stations in Eurasia during 1981–2010 (Figure 1). The climatic scenario data of CMIP5 RCP26, RCP45 and RCP85 scenarios has been got from IPCC website during 2011–2100, and the land cover current data of Eurasia in 2010 has been downloaded from ftp://vct.geog.umd.edu/ST/ (Zhang *et al*., 2016). The mean annual biotemperature, average total annual precipitation and potential evapotranspiration ratio at a spatial resolution of 0.125° × 0.125° were respectively obtained by operating a high accuracy and speed method of surfacing modeling (HASM) (Yue, 2010, Yue *et al*., 2016) during all the four periods 1981 to 2010 (T0), 2011 to 2040 (T1), 2041 to 2070 (T2), and 2071 to 2100 (T3).

The spatial data of biome types at a spatial resolution of 0.125º × 0.125º in T0, T1, T2 and T3 were respectively generated by running the improved Holdridge life zone model, in terms of the spatial data of mean annual biotemperature (MAB), average total annual precipitation (TAP), and potential evapotranspiration ratio (PER) simulated by HASM (Yue *et al*., 2011; Fan *et al*., 2015). The HLZ model (Holdridge 1947, 1967, 1971) is a scheme which utilizes the three bioclimatic variables to formulate the biome distribution (Zhang, 1993; Yue *et al*.,

Figure 1 Location of the weather observation stations in Eurasia

2005, 2006). The HLZ types in Eurasia include Polar/Nival area, Subpolar/Alpine dry tundra, Subpolar/Alpine moist tundra, Subpolar/Alpine wet tundra, Subpolar/Alpine rain tundra, Cold temperate dry scrub, Cold temperate moist forest, Cold temperate wet forest, Cold temperate rain forest, Cool temperate scrub, Cool temperate steppe, Cool temperate moist forest, Cool temperate wet forest, Cool temperate rain forest, Warm temperate desert scrub, Warm temperate thorn steppe, Warm temperate dry forest, Warm temperate moist forest, Warm temperate wet forest, Subtropical desert scrub, Subtropical thorn woodland, Subtropical dry forest, Subtropical moist forest, Subtropical wet forest, Subtropical rain forest, Tropical desert scrub, Tropical thorn woodland, Tropical very dry forest, Tropical dry forest, Tropical moist forest, Tropical wet forest, Tropical rain forest, and Desert (Table 1).

The land cover data of Eurasia have been separated from the land cover data at a spatial resolution of 0.125° × 0.125° of the global rest in 2010. The land cover types were classified into 13 types by combining the land cover classification systems of FAO and UNEP (Gregorio and Jansen, 2001), IGBP, USGS, ESA GlobCover, and UMD, which include Evergreen broadleaf forest, Deciduous broadleaf forest, Evergreen needleleaf forest, Deciduous needleleaf forest, Mixed forest, Shrub land, Grasslands, Wetlands, Croplands, Water bodies, Snow and Ice, Built-up land, Barren or sparsely vegetated land (Table 1).

2.2 Surface modeling of land cover scenarios

Land cover change is a complex process driven by natural factors, climate conditions, and human factors. If the impact of various factors is to be considered in the process of simulated predictive analysis, the entire study will become extremely complicated and it is impossible to start. Climate conditions such as mean annual biotemperature, average total annual precipitation and potential evapotranspiration ratio have directly impact on the natural course of land cover (Lauenroth *et al*., 1993). After comparing the corresponding relationship of the spatial distribution between biome types and land cover types, the distribution of HLZ types and land cover types are very similar on spatial pattern (Fan *et al*., 2005; Yue *et al*., 2007, 2011) (Figure 2). Therefore, SMLCS, as a grid-oriented, spatial explicit land cover scenarios model, has been improved to simulate land cover changes of Eurasia in 2040, 2070 and 2100.

In this paper, the land cover types has been replaced by the relative cover of each land cover type in every cell, e.g. a grid cell includes three land cover types which respectively contain 60% cropland, 25% forest land and 15% grassland, then the land cover data would

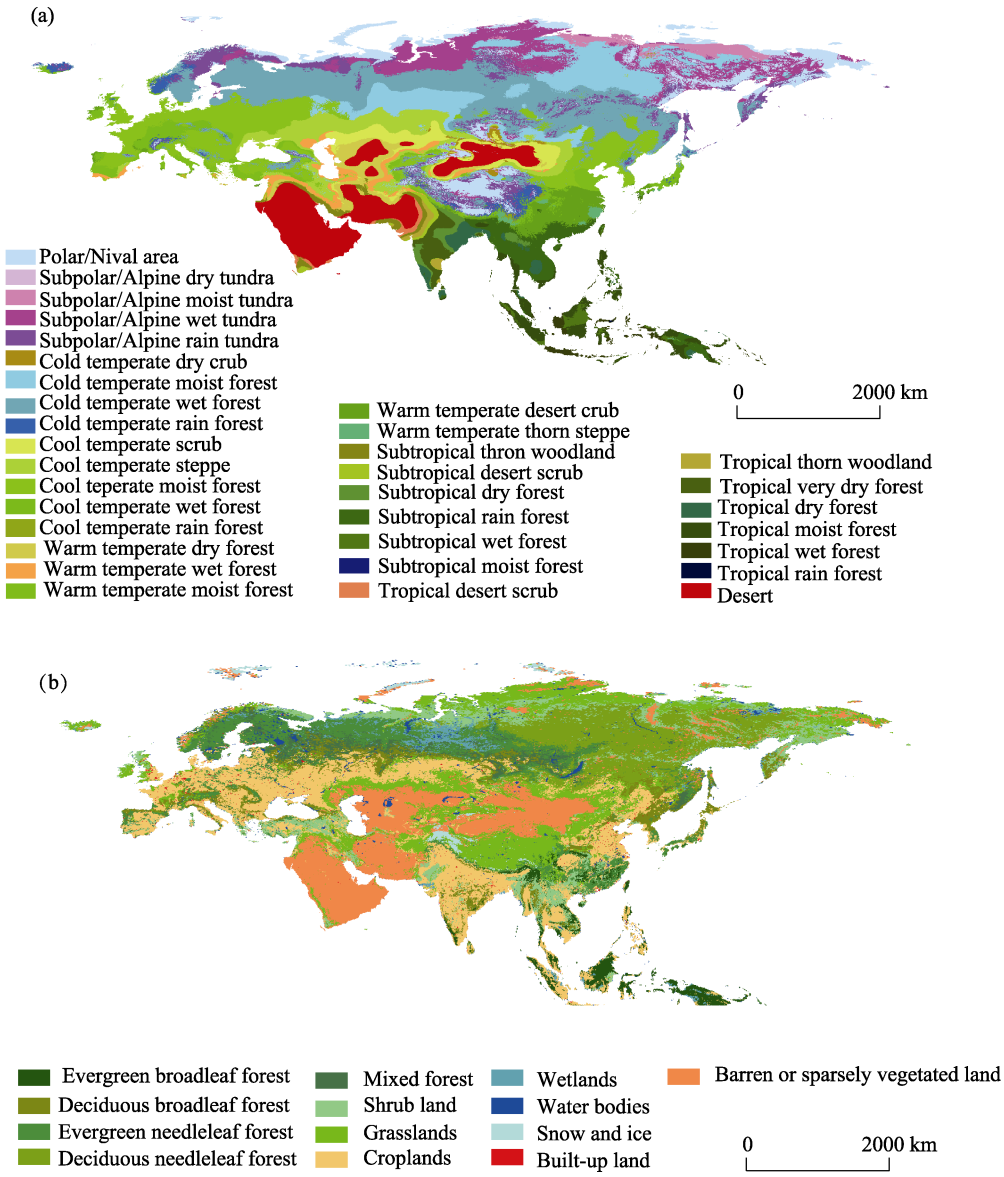

Figure 2 The distribution of HLZ types during 1981–2010 on an average (a) and land cover (b) of Eurasia in 2010

consist of three probability data belonging to three different kinds of land cover types. That is to say, the new transition probability matrix can quantitatively describe the land cover spatial distribution characteristics within each HLZ type (Fan *et al*., 2015). Therefore, land cover type at a grid during next period would tend to the direction that the HLZ type appeared at the grid during next period, e.g. at grid (x, y), if probability of land cover type k corresponding to HLZ type occurred in $t+1$ period is more than that corresponding to HLZ type occurred in t period, the cover probability of land cover type k at the grid would increase. Thus, when we create new probability formulation which indicates the probability of a grid cell to be covered by a certain land cover type, we have to take account the probability

change of each land cover type corresponding to HLZ type between the former and next period. The new probability formulation and decision rules can be formulated as:

$$LP(x,y)_{k,t+1} = LP(x,y)_{k,t} \times \frac{1}{2} \times \left(1 + \frac{HLZP(x,y)_{k,t+1} - HLZP(x,y)_{k,t}}{HLZP(x,y)_{k,t+1} + HLZP(x,y)_{k,t}}\right) \quad (1)$$

$$LC(x,y)_{t+1} = Value(k)_{\max\{LP(x,y)_{k,t+1} | k=1,2,3\ldots\ldots22\}} \quad (2)$$

$$k = 1,2,3\ldots22;\ t = 2010,2040,2070,2100 \quad (3)$$

where x, y is the coordinate of grid cell; k is the type code of land cover; t is the variable of time; $HLZP(x,y)_{k,t}$ represents the transition probability between land cover type k and the HLZ type appeared at grid (x, y) in t year. $LP(x,y)_{k,t}$ is the percentage of land cover type k contained in grid (x, y) which should satisfy the formula $\sum_{k=1}^{22} LP(x,y)_{k,t} = 1$; $LP(x,y)_{k,t+1}$ is the transition probability of land cover type k in t+1 period; $LC(x,y)_{t+1}$ is the type value of land cover at grid (x, y) in t+1 period.

The major steps of the improved SMLCS include: 1) simulating the MAB, TAP and PER data in Eurasia by operating the HASM and simulating the HLZ types distribution by running the HLZ model; 2) establishing the transition probability matrix (Table 1) between HLZ types and land cover types by combining the HLZ type data during 1981–2010 on an average (Figure 2a) and the land cover data in 2010 (Figure 2b); 3) recognizing whether the HLZ type at grid cell (x, y) will change or not from t period to t+1 period; 4) assigning the grid cell (x, y) at t+1 period on the basis of the max value of transition probability; and 5) repeating step 3 and step 4 until all the grid cells of land cover type have been allocated at t+1 period.

3 Results and analyses

3.1 Spatial distribution change of land cover

The simulation results of land cover (Figures 3–5) under the RCP26, RCP45 and RCP85 scenarios show that the spatial distribution of land cover scenario would have a very similar regional change characteristic on the spatial pattern in Eurasia during 2010–2100. There would be a great difference in spatial distribution of forest and shrub because of the complicated terrain characteristics and heterogeneous climate change in Eurasia. Evergreen broadleaf forest would be mostly distributed in Southeast Asia. Evergreen needleleaf forest would mainly be distributed in Nordic Europe, East European Plain, Western Siberian Plain, Japan, South Korea, and hilly areas in South China. Deciduous needleleaf forest would be mainly distributed in Central Siberian Highlands and Eastern Siberia, which would cover about half of Russia's area. Shrub land would be mainly distributed in the north and east of Russia, southwest China, northeast Laos, the border zone between India and Myanmar and the border zone between India and Pakistan, the north of United Kingdom, the south of Greece, most of Turkey, east of Georgia, and central Azerbaijan.

Table 1 Transition probability matrix from HLZ types in T0 on an average to land cover types in 2010

HLZ type code	Land cover type code												
	Evergreen broadleaf forest	Deciduous broadleaf forest	Evergreen needleleaf forest	Deciduou snee-dleleaf forest	Mixed forest	Shrub land	Grass-lands	Wetlands	Croplands	Water bodies	Snow and ice	Built-up land	Barren or sparsely vege-tated land
Polar/Nival area	0	0.03	0.25	0.43	0.01	1.82	7.61	0.07	0	0.74	87.61	0	1.42
Subpolar/Alpine dry tundra	0	0	0	2.27	0	0	87.5	0	1.14	2.27	3.41	0	3.41
Subpolar/Alpine moist tundra	0	0	0	12.69	0	12.85	51.73	3.18	0.04	4.74	11.12	0	3.65
Subpolar/Alpine wet tundra	0	0.16	5.51	17.09	0.36	23.62	42.73	2.64	0.13	4	1.33	0	2.43
Subpolar/Alpine rain tundra	0.05	2.64	28.88	9.6	2.16	15.45	27.9	1.69	0.42	3.71	4.11	0.01	3.37
Cold temperate dry scrub	0	0	0.05	2.43	0	0.52	19.51	0.05	3.34	2.91	17.13	0	54.06
Cold temperate moist forest	0	5.69	8.58	37.03	4.35	10.34	14.53	1.42	11.6	2.78	0.2	0.06	3.42
Cold temperate wet forest	0.01	8.62	33.14	14.15	13.02	7.95	7.26	3.95	4.96	4.07	0.38	0.07	2.42
Cold temperate rain forest	2.07	5.29	33.63	0.02	6.89	5.25	32.6	0.98	1.05	5.12	4.92	0.01	2.18
Cool temperate scrub	0.08	0.03	0.44	0	0.02	2.17	22.79	0.08	1.92	1.66	0.05	0	70.76
Cool temperate steppe	0.01	0.51	3.2	0.05	0.09	12.43	40.94	0.12	28.6	1.45	0.01	0.17	12.43
Cool temperate moist forest	0.34	8.23	8.56	0.49	2.91	9.91	17.95	0.12	46.49	3.53	0.03	0.33	1.11
Cool temperate wet forest	3.33	22.49	15.46	0	10.77	4.05	10.72	0.19	25.66	5.71	0.17	0.71	0.74
Cool temperate rain forest	23.62	5.16	13.63	0	6.35	1.35	34.97	0	1.1	11.77	1.1	0	0.93
Warm temperate desert scrub	0.45	0.1	1.22	0	0	3.73	14.95	0	5.77	2.2	0	0.04	71.54
Warm temperate thorn steppe	0.95	4.61	3.09	0	0.19	25.53	31.57	0.08	12.91	0.89	0	0.08	20.1
Warm temperate dry forest	4.82	4.25	8.33	0	0.4	20.86	21.14	0.47	36.87	1.31	0	0.26	1.29
Warm temperate moist forest	7.88	12.34	16.87	0	3.07	9.33	7.12	0.02	41.16	1.64	0.02	0.51	0.03
Warm temperate wet forest	37.37	0.47	17.69	0	5.57	7.1	6.31	0	24.9	0.43	0	0	0.16

(*To be continued on the next page*)

(***Continued***)

HLZ type code	Land cover type code												
	Evergreen broadleaf forest	Deciduous broadleaf forest	Evergreen needleleaf forest	Deciduou snee-dleleaf forest	Mixed forest	Shrub land	Grass-lands	Wetlands	Croplands	Water bodies	Snow and ice	Built-up land	Barren or sparsely vege-tated land
Subtropical desert scrub	0.38	0.44	0.69	0	0	9.99	18.75	0.44	16.69	1.2	0	0.3	51.14
Subtropical thorn woodland	1.57	2.55	0.67	0	0.02	8.98	59.79	0.91	12.34	1.48	0	0.17	11.5
Subtropical dry forest	4.75	16.76	2.26	0	0.3	24.2	24.15	1.07	24.12	1.82	0	0.11	0.45
Subtropical moist forest	24.59	22.71	4.24	0	0.05	12.52	6.26	1.65	25.94	1.87	0	0.12	0.04
Subtropical wet forest	66.49	0.93	1.03	0	0	5.08	3.86	0.79	20.67	1.17	0	0	0
Subtropical rain forest	80	0	0	0	0	0	0	0	20	0	0	0	0
Tropical desert scrub	0	0.2	0	0	0	1.14	8.13	0.94	9.22	0.32	0	0.02	80.02
Tropical thorn woodland	1.1	1.6	0	0	0	1.03	36.47	0.35	19.1	0.89	0	0.1	39.35
Tropical very dry forest	17.9	5.51	0.12	0	0.03	6.53	39.78	1.06	25.06	1.44	0	0.07	2.51
Tropical dry forest	25.79	13.23	0.2	0	0.11	17.8	6.09	2.41	31.94	2.07	0	0.09	0.27
Tropical moist forest	66.93	1.55	0.01	0	0	3.85	2.33	4.98	18.55	1.74	0	0.06	0
Tropical wet forest	44.83	0	0	0	0	1.04	2.27	4.42	38.56	8.55	0	0.33	0
Tropical rain forest	93.75	0	0	0	0	0	0	0	3.13	3.13	0	0	0
Desert	0	0.01	0.08	0	0	1.74	3.38	0.04	3.13	0.43	0.01	0.05	91.13

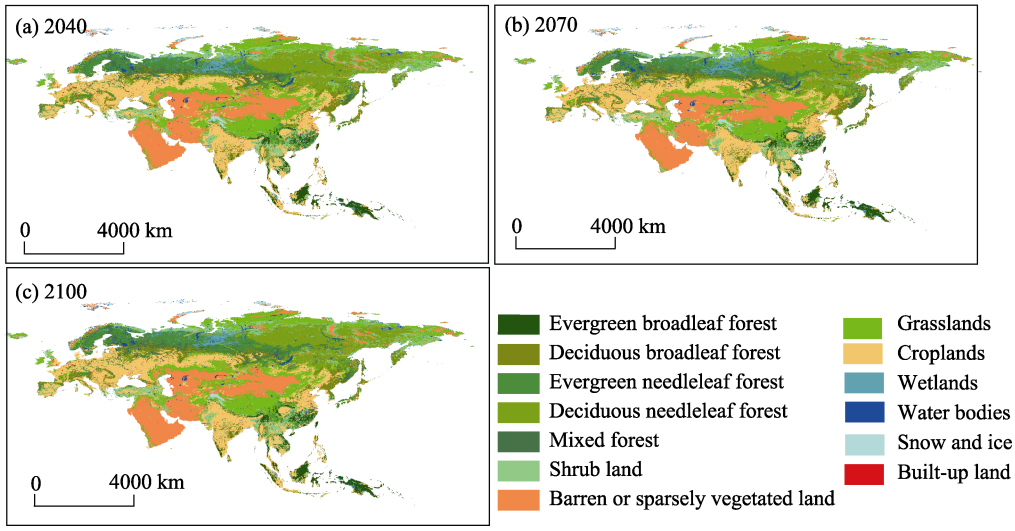

Figure 3 RCP26 scenario of land cover change in Eurasia

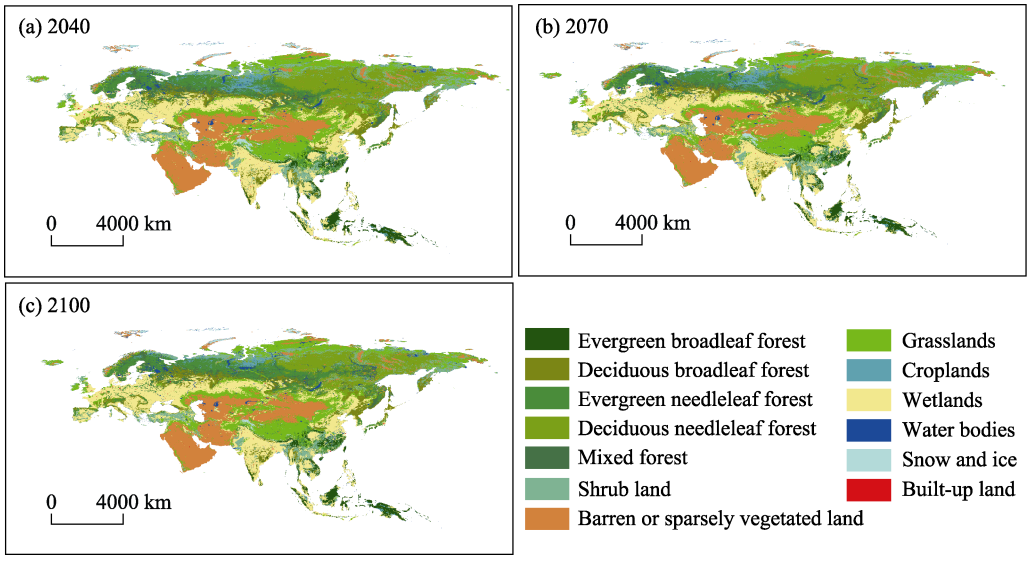

Figure 4 RCP45 scenario of land cover change in Eurasia

Grasslands would mainly be distributed in Tianshan Mountains, Tibetan Plateau, Inner Mongolian Plateau, Loess Plateau, Altai Mountains and areas around Tarim Basin of China, North Siberian Plain, Norway, the northwest of Iran, the north of Kazakhstan and the middle of Mongolia.

Croplands would mainly be distributed in the East European and Central European Plains. Croplands would mainly be distributed in Northeast China Plain, North China Plain, middle and lower reaches of the Yangtze River, Sichuan Basin and Guanzhong Basin of China. Hexi Corridor and the river alluvial sectors of Tianshan Mountains in China also would have relatively concentrated cultivated land. The centre of South Asia is one of the greatest alluvial plains in the world, which is formed by Indus, Ganges and Brahmaputra rivers, with dense river networks, numerous irrigation channels, and developed agriculture, such as India. In addi-

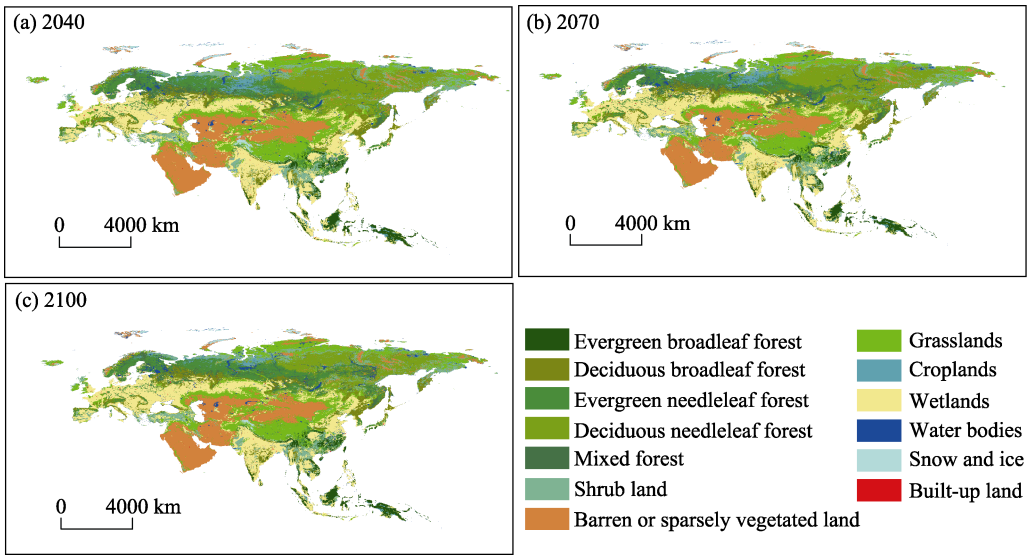

Figure 5 RCP85 scenario of land cover change in Eurasia

tion, croplands would be mainly distributed in Thailand, Myanmar, Vietnam in IndoChinese Peninsula, the coastal area of Malay Archipelago.

Barren or sparsely vegetated land would mainly be distributed in Uzbekistan, Turkmenistan and southern Kazakhstan of Central Asia, and Iran, Saudi Arabia, Yemen of Western Asia. Moreover, barren or sparsely vegetated land would be distributed in southern Mongolia and Northwest China. In China, barren or sparsely vegetated land would mainly be distributed in the arid and desert areas in the northwest, namely Gurbantunggut Desert in Junggar Basin, Taklimakan Desert in Tarim Basin, the center of Qaidam Basin, and Tengger Desert, Alax Plateau.

Water bodies include rivers and lakes. The main water body area is river area, which include Volga River, Yenisei, Ob River, Ural River, Syr Darya, Tigris River, Euphrates River, Po, and Mekong. Lakes would mainly be distributed in Finland, named Country of Thousand Lakes that mainly include Baikal, and Aral Sea. In China, the river system mainly originates from Qilian and Hengduan mountains in the east of the Qinghai-Tibet Plateau, the mountainous areas around the Sichuan Basin, the Changbai Mountains in the northeast, the Greater Xinggan Mountains, and the hilly regions in South China. The distribution of water bodies would be more dispersed than other land cover types. Wetlands would mainly be distributed in Western Siberian Plain.

Snow and ice would mainly be distributed in the Himalayas, the high latitude zone in Nordic Europe and North Asia. Built-up land would mainly be distributed in areas that would be close to rivers, sufficient water resources, convenient to transport, fertile land and rich products, due to the formation and development factors of urban and the land use characteristics of artificial land.

3.2 Area changes of land cover types

During 2010–2100, the area of evergreen broadleaf forest, grasslands, croplands, water bodies and built-up land would increase while the areas of deciduous needleleaf forest and snow and ice would decrease under all three scenarios of RCP26, RCP45 and RCP85 (Tables 2–4)

in all the three periods. The area of deciduous broadleaf forest would increase in all the three periods under all the scenarios except a decrease during 2010–2040 under the RCP26 scenario. The area of mixed forest and shrub land would decrease in all the three periods under the RCP26 scenario, which would increase during 2070–2100 under the two scenarios of RCP45 and RCP 85. Compared with 2010, the area of deciduous broadleaf forest, mixed forest, shrub land and wetlands would decrease in 2100 under all three scenarios. The area of wetlands would increase during 2010–2040 and then decrease during 2040–2100 under the two scenarios of RCP45 and RCP85, but which would increase from 2010 to 2070 and then decrease from 2070 to 2100 under the RCP26 scenario. The area of evergreen needleleaf forest would decrease during 2010–2070 and increase during 2070–2100 under the two scenarios of RCP26 and RCP45. But under the RCP85 scenario, the area of evergreen needleleaf forest would decrease during 2010–2040 and then increase during 2040–2100.

The area of barren or sparsely vegetated land would decrease during 2010–2040 and then increase during 2040–2100 under the two scenarios of RCP45 and RCP85, but it would decrease during 2010–2070 and then increase during 2070–2100 under the RCP 26 scenario.

In terms of the simulated results of land cover under the three scenarios of RCP26, RCP45 and RCP85 (Tables 2–7), most land cover types would generally have similar changing trends in the future, but which have some difference in different periods.

During 2010–2040: shrub land would have the greatest decrease area, down respectively by 187,409 km^2 and 146,044 km^2 under the two scenarios of RCP26 and RCP45, and evergreen needleleaf forest would have the greatest decrease area, down by 154,486 km^2 under the scenario RCP85; snow and ice would have the largest decrease rate, down respectively by 7.55% and 7.65% under the two scenarios of RCP26 and RCP45, and mixed forest would have the largest decrease rate, down by 9.50% under the scenario of RCP85; croplands would all have the greatest increase area, up by 318,257 km^2, 282,168 km^2 and 261,486 km^2, respectively, and wetlands would all have the largest increase rate, up by 6.56%, 6.98% and 7.31% under the three scenarios of RCP26, RCP45 and RCP85, respectively.

Table 2 Area of land cover type based on RCP26 (km^2)

Land cover type	2010	2040	2070	2100	Area change	Change rate (%)
Evergreen broadleaf forest	2363080	2482321	2549012	2635963	272882	11.55
Deciduous broadleaf forest	3268045	3256437	3354152	3400582	132537	4.06
Evergreen needleleaf forest	4677409	4537064	4478604	4527778	–149632	–3.20
Deciduous needleleaf forest	4796439	4715819	4564922	4298793	–497646	–10.38
Mixed forest	1576935	1484708	1399023	1376441	–200494	–12.71
Shrub land	4265659	4078250	4023800	3973782	–291876	–6.84
Grasslands	8752493	8785628	8857383	8962695	210202	2.40
Wetlands	907075	966590	969967	892091	–14984	–1.65
Croplands	12226519	12544776	12692297	12748647	522127	4.27
Water bodies	862333	892091	930923	986850	124517	14.44
Snow and Ice	416393	384948	344849	311926	–104468	–25.09
Built-up land	222231	225397	228141	230040	7809	3.51
Barren or sparsely vegetated land	9747152	9727736	9688693	9736178	–10974	–0.11

Table 3 Area of land cover type based on RCP45 (km^2)

Land cover type	2010	2040	2070	2100	Area change	Change rate (%)
Evergreen broadleaf forest	2363080	2453619	2572016	2685347	322267	13.64
Deciduous broadleaf forest	3268045	3280286	3365759	3487322	219277	6.71
Evergreen needleleaf forest	4677409	4537486	4523135	4777445	100036	2.14
Deciduous needleleaf forest	4796439	4770058	4511738	3635687	–1160752	–24.20
Mixed forest	1576935	1478165	1363145	1405776	–171158	–10.85
Shrub land	4265659	4119615	3995520	4024644	–241014	–5.65
Grasslands	8752493	8774231	8879543	9153058	400565	4.58
Wetlands	907075	970389	954982	725154	–181922	–20.06
Croplands	12226519	12508687	12679001	12772284	545765	4.46
Water bodies	862333	888925	954138	1106302	243969	28.29
Snow and Ice	416393	384526	343583	254732	–161661	–38.82
Built-up land	222231	225608	228563	232150	9919	4.46
Barren or sparsely vegetated land	9747152	9690170	9710642	9821863	74710	0.77

Table 4 Area of land cover type based on RCP85 (km^2)

Land cover type	2010	2040	2070	2100	Area change	Change rate (%)
Evergreen broadleaf forest	2363080	2451298	2603673	2746340	383259	16.22
Deciduous broadleaf forest	3268045	3294215	3463473	3503994	235949	7.22
Evergreen needleleaf forest	4677409	4522924	4554158	4895208	217799	4.66
Deciduous needleleaf forest	4796439	4783565	4405371	3232589	–1563850	–32.60
Mixed forest	1576935	1427092	1263320	1275772	–301162	–19.10
Shrub land	4265659	4136499	3979058	4133755	–131904	–3.09
Grasslands	8752493	8763679	8958474	9317041	564548	6.45
Wetlands	907075	973343	856002	636725	–270350	–29.80
Croplands	12226519	12488005	12645656	12802252	575733	4.71
Water bodies	862333	897789	1002046	1190721	328387	38.08
Snow and Ice	416393	386425	310237	227296	–189097	–45.41
Built-up land	222231	226874	231306	232995	10763	4.84
Barren or sparsely vegetated land	9747152	9730058	9808989	9887076	139923	1.44

During 2040–2070: deciduous needleleaf forest would all have the greatest decrease area, down respectively by 150,898 km^2, 258,320 km^2 and 378,194 km^2, snow and ice would all have the largest decrease rate, down respectively by 10.42%, 10.65% and 19.72%, and water bodies would all have the largest increase rate, up by 4.35%, 7.34% and 11.61% under the three scenarios of RCP26, RCP45 and RCP85, respectively; croplands would have the greatest increase area, up by 147,521 km^2 and 170,314 km^2 under the two scenarios of RCP26 and RCP45, respectively; grasslands would have the greatest increase area that would be 194,795 km^2 un der the scenario RCP85.

During 2070–2080: under the three scenarios of RCP26, RCP45 and RCP85, deciduous needleleaf forest would all have the greatest decrease area, down respectively by 266,129 km^2, 876,051 km^2 and 1,172,782 km^2; snow and ice would all have the largest decrease rate, down

Table 5 Scenario of land cover change based on RCP26 (km^2)

Land cover type	From 2011 to 2040		From 2041 to 2070		From 2071 to 2100	
	Area	Change rate (%)	Area	Change rate (%)	Area	Change rate (%)
Evergreen broadleaf forest	119241	5.05	66690	2.69	86951	3.41
Deciduous broadleaf forest	–11608	–0.36	97714	3.00	46430	1.38
Evergreen needleleaf forest	–140345	–3.00	–58460	–1.29	49174	1.10
Deciduous needleleaf forest	–80620	–1.68	–150898	–3.20	–266129	–5.83
Mixed forest	–92227	–5.85	–85685	–5.77	–22582	–1.61
Shrub land	–187409	–4.39	–54450	–1.34	–50018	–1.24
Grasslands	33134	0.38	71756	0.82	105312	1.19
Wetlands	59515	6.56	3377	0.35	–77876	–8.03
Croplands	318257	2.60	147521	1.18	56349	0.44
Water bodies	29757	3.45	38832	4.35	55927	6.01
Snow and Ice	–31446	–7.55	–40099	–10.42	–32923	–9.55
Built-up land	3166	1.42	2744	1.22	1899	0.83
Barren or sparsely vegetated land	–19416	–0.20	–39043	–0.40	47485	0.49

Table 6 Scenario of land cover change based on RCP45 (km^2)

Land cover type	From 2011 to 2040		From 2041 to 2070		From 2071 to 2100	
	Area	Change rate (%)	Area	Change rate (%)	Area	Change rate (%)
Evergreen broadleaf forest	90539	3.83	118397	4.83	113332	4.41
Deciduous broadleaf forest	12241	0.37	85474	2.61	121562	3.61
Evergreen needleleaf forest	–139923	–2.99	–14351	–0.32	254310	5.62
Deciduous needleleaf forest	–26381	–0.55	–258320	–5.42	–876051	–19.42
Mixed forest	–98769	–6.26	–115020	–7.78	42631	3.13
Shrub land	–146044	–3.42	–124095	–3.01	29124	0.73
Grasslands	21738	0.25	105312	1.20	273515	3.08
Wetlands	63314	6.98	–15406	–1.59	–229829	–24.07
Croplands	282168	2.31	170314	1.36	93282	0.74
Water bodies	26592	3.08	65213	7.34	152164	15.95
Snow and Ice	–31868	–7.65	–40943	–10.65	–88850	–25.86
Built-up land	3377	1.52	2955	1.31	3588	1.57
Barren or sparsely vegetated land	–56982	–0.58	20471	0.21	111221	1.15

respectively by 9.55%, 25.86% and 26.73%; grasslands would all have the greatest increase area, up respectively by 105,312 km^2, 273,515 km^2 and 358,567 km^2; water bodies would all have the largest increase rate, up respectively by 6.01%, 15.95% and 18.83%.

During 2010–2100, deciduous needleleaf forest would all have the greatest decrease area, down by 497,646 km^2, 1,160,752 km^2 and 1,563,850 km^2, respectively. Snow and ice would all have the largest decrease rate, being 25.09%, 38.82% and 45.51%, respectively. Croplands would all have the greatest increase area, up by 522,127 km^2, 545,765 km^2 and 575,733 km^2, respectively. Water bodies would all have the largest increase rate, being 14.44%, 28.29% and 38.08%, respectively.

Table 7 Scenario of land cover change based on RCP85 (km^2)

Land cover type	From 2011 to 2040		From 2041 to 2070		From 2071 to 2100	
	Area	Change rate (%)	Area	Change rate (%)	Area	Change rate (%)
Evergreen broadleaf forest	88217	3.73	152375	6.22	142667	5.48
Deciduous broadleaf forest	26170	0.80	169259	5.14	40521	1.17
Evergreen needleleaf forest	–154486	–3.30	31235	0.69	341050	7.49
Deciduous needleleaf forest	–12874	–0.27	–378194	–7.91	–1172782	–26.62
Mixed forest	–149843	–9.50	–163772	–11.48	12452	0.99
Shrub land	–129160	–3.03	–157440	–3.81	154697	3.89
Grasslands	11185	0.13	194795	2.22	358567	4.00
Wetlands	66268	7.31	–117341	–12.06	–219277	–25.62
Croplands	261486	2.14	157651	1.26	156596	1.24
Water bodies	35456	4.11	104257	11.61	188675	18.83
Snow and Ice	–29969	–7.20	–76188	–19.72	–82941	–26.73
Built-up land	4643	2.09	4432	1.95	1688	0.73
Barren or sparsely vegetated land	–17095	–0.18	78931	0.81	78087	0.80

4 Conclusions and discussion

4.1 Conclusions

The simulated results of land cover under the three scenarios RCP26, RCP45 and RCP85 indicate that deciduous needleleaf forest, mixed forest, shrub land, wetlands and snow and ice would generally decrease in Eurasia during 2010–2100. Snow and ice would have the fastest decreasing rate that would decrease by 36.44% on average. Shrub land would have the slowest decreasing rate that would decrease by 5.19% on average. Water bodies would have the fastest increasing rate that would increase by 26.94% on average. Barren or sparsely vegetated land would have the slowest increasing rate that would increase by 0.70%. Further more, the simulation results show that there would generally appear a similar change pattern of land cover driven by different levels of climate change scenarios in Eurasia. Land cover under the RCP85 scenario would generally have the fastest change rate, especially that the reducing trend of snow and ice would be much faster than that of scenarios of RC26 and RC45. There would have the lowest change rate of land cover in the scenario RCP26. The simulated results can approve proofs that climate change would directly impact on land cover change in Eurasia. For instance, the RCP85 is a highly energy-intensive scenario as a result of high population growth, a lower rate of technology development and non-climate policy, which represent a high scenario in climate change. Under the RC85 scenario, the temperature and precipitation would have the faster increase rate than other two scenarios of RCP26 and RCP45, so that there would have the largest change rate of land cover simulated by using the climatic data of the scenario RCP85. With the rapid increase of temperature and precipitation, the snow and ice would have a fast melting trend, the grasslands would also show an increasing trend, and the succession would occur between different forest types.

4.2 Discussion

HLZ model can simulate long-term biome types, so SMLCS can also be used to simulate land cover types at long-term scale (Fan *et al*., 2013, 2015). In this paper, the aim of improved SMLCS is that can be used to simulate land cover change from the perspective of climate change because there is not enough socioeconomic data and human activities data in Eurasia. However, with the advance of the Belt and Road initiative, we believe that lots of socioeconomic data and human activities data would can be collected from more data sources, so in our future work, more parameter data will be considered into the next improved SMLCS which would include the agricultural pattern, population density, road construction, and government policy, etc. That is to say, we will focus on analyzing and discussing what is the coupling effect of climate change and human activities on land cover change, and then further improve the SMLCS.

Moreover, with the driving force and influence of climate change and human activities, the spatiotemporal distribution pattern of land cover in Eurasia has obviously changed since the beginning of the 21st century. How to understand and explain the land cover change is an important issue in the implementation of the Belt and Road Initiative. The current simulation results can reflect the land cover change scenarios driven by climate change, and can also provide the land cover data for the study of hydrological cycle, soil erosion and biological diversity in the context of climate change in Eurasia. We believed that further simulated results by operating the future improved SMLCS combined with human activities and policy factors will approve the more important data for supporting a series of major projects about the Belt and Road Initiative.

References

Adams R M, Fleming R A, Chang C C *et al*., 1995. A reassessment of the economic effects of global climate change on U.S. agriculture. *Climatic Change*, 30(2): 147–167.

Alcamo J, Kreileman G J J, Krol M S *et al*., 1994. Modeling the global society-biosphere-climate system: Part 1: Model description and testing. *Water Air & Soil Pollution*, 76(1/2): 1–35.

Bai W Q, Zhang Y M, Yan J Z, 2005. Simulation of land use dynamics in the upper reaches of the Dadu River. *Geographical Research*, 24(2): 206–212. (in Chinese)

Clarke K, Hoppen S, Gaydos L, 1997. A self-modifying cellular automaton model of historical urbanization in the San Francisco Bay area. *Environment & Planning B Planning & Design*, 24(2): 247–261.

Fan Z M, Li J Y, Yue T X, 2013. Land-cover changes of biome transition zones in Loess Plateau of China. *Ecological Modelling*, 252: 129–140.

Fan Z M, Li J Y, Yue T X *et al*., 2015. Scenarios of land cover in karst area of southwestern China. *Environmental Earth Sciences*, 74(8): 6407–6420.

Fan Z M, Yue T X, Liu J Y *et al*., 2005. Spatial and temporal distribution of land cover scenarios in China. *Acta Geographica Sinica*, 60(6): 941–952. (in Chinese)

Fan Z M, Zhang X, Jing Li *et al*., 2013. Land-cover changes of national nature reserves in China. *Journal of Geographical Sciences*, 23(2): 258–270.

Fischer G, Ermoliev Y M, Keyzer M A *et al*., 1996. Simulating the socio-economic and biogeographical driving forces of land-use and land cover change: The IIASA land-use change model. IIASA Working Paper, WP-96-010.

Gao Z Q, Yi W, 2012. Land use change in China and analysis of its driving forces using CLUE-S and Dinamica EGO model. *Chinese Society of Agricultural Engineering*, 28(16): 208–216. (in Chinese)

Gregorio A D, Jansen L J M, 2001. Land cover classification system (LCCS): Classification concepts and user manual for software version 1.0. FAO.

Guo Y F, Yu X B, Jiang L G *et al*., 2012. Scenarios analysis of land use change based on CLUE model in Jiangxi

Province by 2030. *Geographical Research*, 31(6): 1016–1028. (in Chinese)
He C Y, Chen J, Shi P J *et al*., 2002. Study on the spatial dynamic city model based on CA (Cellular Automata) model. *Progress in Geography*, 21(2): 188–119. (in Chinese)
Holdridge L R, 1947. Determination of world plant formations from simple climate data. *Science*, 105(2727): 367.
Holdridge L R, 1967. Life Zone Ecology. Libros Y Materiales Educativos.
Holdridge L R, Grenke W C, Hatheway W H *et al*., 1971. Forest Environments in Tropical Life Zones. Oxford: Pergamon Press.
Ichinose T, Otsubo K, 2003. Temporal structure of land use change in Asia. *Journal of Global Environment Engineering*, 9: 41–51.
Lauenroth W K, Urban D L, Coffin D P *et al*., 1993. Modeling vegetation structure-ecosystem process interactions across sites and ecosystems. *Ecological Modelling*, 67(1): 49–80.
Li J, Fan Z M, Yue T X, 2014. Spatio-temporal simulation of land cover scenarios in southwestern of China. *Acta Ecologica Sinica*, 34(12): 3266–3275. (in Chinese)
Li X, Yu L, Sohl T *et al*., 2016. A cellular automata downscaling based 1 km global land use datasets (2010–2100). *Science Bulletin*, 61(21): 1651–1661.
Turner B L I, Skole D L, Sanderson S *et al*., 1995. Land-use and land-cover change, Science/research plan. *Global Change Report*, 43: 669–679.
Veldkamp A, Fresco L O, 1996. CLUE: A conceptual model to study the conversion of land use and its effects. *Ecological Modelling*, 85(2): 253–270.
Verburg P H, 2000. Exploring the spatial and temporal dynamics of land use with special reference to China. Wageningen University.
Verburg P H, Schot P P, Dijst M J *et al*., 2004. Land use change modeling: Current practice and research priorities. *GeoJournal*, 61(4): 309–324.
Verburg P H, Soepboer W, Veldkamp A *et al*., 2002. Modeling the spatial dynamics of regional land use: The CLUE-S Model. *Environmental Management*, 30(3): 391–405.
Verburg P H, Veldkamp A, Fresco L O, 1999. Simulation of changes in the spatial pattern of land use in China. *Applied Geography*, 19(3): 211–233.
Vuuren D P V, Edmonds J, Kainuma M *et al*., 2011. The representative concentration pathways: An overview. *Climatic Change*, 109(1/2): 5.
Wu F, 2002. Calibration of stochastic cellular automata: The application to rural-urban land conversions. *International Journal of Geographical Information Systems*, 16(8): 795–818.
Wu F, Webster C J, 1998. Simulation of land development through the integration of cellular automata and multicriteria evaluation. *Environment & Planning B Planning & Design*, 25(1): 103–126.
Yue T X, 2010. Surface Modeling: High Accuracy and High Speed Methods. Boca Raton: CRC Press.
Yue T, Fan Z, Chen C *et al*., 2011. Surface modelling of global terrestrial ecosystems under three climate change scenarios. *Ecological Modelling*, 222(14): 2342–2361.
Yue T X, Fan Z M, Liu J Y, 2005. Changes of major terrestrial ecosystems in China since 1960. *Global and Planetary Change*, 48: 287–302.
Yue T X, Fan Z M, Liu J Y *et al*., 2006. Scenarios of major terrestrial ecosystems in China. *Ecological Modelling*, 199: 363–376.
Yue T X, Fan Z M, Liu J Y, 2007. Scenarios of land cover in China. *Global and Planetary Change*, 55(4): 317–342.
Yue T X, Wang Y A, Liu J Y *et al*., 2005. Surface modelling of human population distribution in China. *Ecological Modelling*, 181(4): 461–478.
Yue T X, Zhao N, Douglas Ramsey R *et al*., 2013. Climate change trend in China, with improved accuracy. *Climatic Change*, 120: 137–151.
Yue T X, Zhao N, Fan Z M *et al*., 2016. CMIP5 downscaling and its uncertainty in China. *Global and Planetary Change*, 146: 30–37.
Yue T X, Zhao N, Yang H *et al*., 2013. A multi-grid method of high accuracy surface modeling and its validation. *Transaction in GIS*, 17(6): 943–952.
Zhang R, Huang C Q, Zhan X *et al*., 2016. Development and validation of the global surface type data product from S-NPP VIIRS. *Remote Sensing Letters*, 7: 1, 51–60.
Zhang X S, 1993. A vegetation-climate classification system for global change studies in China. *Quaternary Sciences*, 13(2): 157–169. (in Chinese)